



# Chemically modified novel PAMAM-ZnO nanocomposite: Synthesis, characterization and photocatalytic activity



Balu Krishnakumar<sup>a</sup>, Toyoko Imae<sup>a,b,\*</sup>

<sup>a</sup> Graduate Institute of Applied Science and Technology, National Taiwan University of Science and Technology, 43 Section 4, Keelung Road, Taipei 10607, Taiwan

<sup>b</sup> Department of Chemical Engineering, National Taiwan University of Science and Technology, 43 Section 4, Keelung Road, Taipei 10607, Taiwan

## ARTICLE INFO

### Article history:

Received 28 May 2014

Received in revised form 25 July 2014

Accepted 9 August 2014

Available online 17 August 2014

### Keywords:

ZnO nano rod

Poly(amido amine) dendrimer

Dendrimer-ZnO nanocomposite

Photodegradation

Naphthol blue black

## ABSTRACT

In this paper, for the first time, chemically modified dendrimer-ZnO nanocomposite was prepared and used for the photodegradation of an azo dye naphthol blue black (NBB) under UV light. Initially, ZnO was prepared by simple physical grinding of zinc acetate with sodium hydroxide under solvent free condition. The chemical modification of ZnO was carried out by binding poly(amido amine) (PAMAM) dendrimer through glycidoxypolytrimethoxy silane as a binding agent. The formation of rod like dendrimer-ZnO nanocomposite was confirmed by different characterization techniques. The photocatalytic activity was highly influenced by initial pH of dye solutions. This catalyst was reusable.

© 2014 Elsevier B.V. All rights reserved.

## 1. Introduction

Semiconductor photocatalysis is one of the potential methods for environmental purification and converting photon energy into chemical energy [1–4]. A main drawback to achieve high photocatalytic efficiency is the rapid recombination of photo-generated electron–hole pairs. Therefore, to enhance the photocatalysis efficiency, it is essential to retard the recombination of the electron–hole pairs. Many works have been devoted to achieve the high photocatalytic efficiency by coupling the photocatalysts with other materials, such as noble metals [5,6], semiconductors [3,7], carbon dot [8], etc.

Dendrimers are synthetic macromolecules with a dendritic structure. Especially, poly(amido amine) (PAMAM) dendrimer of the fourth generation (G4) with an ethylenediamine core can be used as convenient dendritic nanocarriers for carrying molecules including biological drugs and genes [9,10] on account of its size (diameter: 4.5–5 nm) [11,12], spherical shape [13] and the presence of functional groups analogous to those occurring in biomolecules

[14] (that is, 124 amide groups, 62 tertiary amine groups, 64 apparent primary amine groups) [15]. PAMAM dendrimer had also been used as biosensors combined with platinum nanoparticles and carbon nanotubes [16], and TiO<sub>2</sub> protected by dendrimer was used for the degradation of 2,4-dichlorophenoxyacetic acid [2]. In the present study, we have chosen ZnO as a base material.

ZnO is known to be one of the important photocatalysts because of its many advantages, such as low price, large initial rates of activities, many active sites with high surface reactivity, high absorption efficacy of light radiations, and environmental safety. The energy levels for the conduction and valence bands, the chemical properties and the electron affinity of ZnO are similar to those of TiO<sub>2</sub>, making ZnO a likely candidate as a semiconductor material for photocatalysis. It is also anticipated that ZnO can become a versatile alternative to TiO<sub>2</sub> [17–19], since some researchers have mentioned that ZnO is much more efficient than TiO<sub>2</sub>, particularly, on photocatalytic degradations of azo dyes [18–20]. ZnO is one of the most important n-type semiconductor materials with a 3.37 eV band gap at room temperature and a 60 meV excitation banding energy [21] that is in the UV region and makes this nanoparticle an efficient UV absorber [22].

However, ZnO also has several drawbacks, including the fast recombination of the photogenerated electron–hole pair and a low quantum yield in the photocatalytic reactions in aqueous solutions, which obstruct the commercialization of ZnO for photocatalytic degradation. In order to improve photocatalytic activity of ZnO,

\* Corresponding author at: Graduate Institute of Applied Science and Technology, National Taiwan University of Science and Technology, 43 Section 4, Keelung Road, Taipei 10607, Taiwan. Tel.: +886 2 2730 3627; fax: +886 2 2730 3627.

E-mail addresses: [imae@mail.ntust.edu.tw](mailto:imae@mail.ntust.edu.tw), [spsm3xn9@citrus.ocn.ne.jp](mailto:spsm3xn9@citrus.ocn.ne.jp) (T. Imae).

several methods have been developed [3,5,23–25]. For this reason, reactive silane coupling agents have often been used as they can form stable chemical bonds between both inorganic (metal oxide) and organic materials. To date, literatures related to surface functionalization of metal oxides have largely been focused on silica particles [26,27], and some molecular treatments of ZnO particles have been investigated [28,29].

Therefore, in the present investigation, for the first time, the surface of ZnO prepared by simple physical grinding was chemically modified by PAMAM dendrimer using glycidoxypropyltrimethoxy silane (GPTMS) as a binding agent. The chemical modification of particle (ZnO) surface, which can be classified as surface grafting, is the most promising method because of the strong covalent bond between particle surface and PAMAM dendrimer. The surface modification reduces its surface energy and hence the agglomeration, resulting in the dispersibility of ZnO particles. To the best of our knowledge, this is the first report on the synthesis of chemically modified dendrimer-ZnO nanocomposite and its use in the degradation of naphthol blue black (NBB) dye under UV light illumination.

## 2. Experimental

### 2.1. Materials

Zinc acetate dihydrate (99%) and sodium hydroxide were obtained from Acros Chemicals. A 10 wt% methanol solution of fourth generation (G4) amine-terminated PAMAM dendrimer, glycidoxypropyltrimethoxy silane (GPTMS), and azo dye NBB (the structure of the dye and its absorption maxima are given in Figure S1, see Supplementary data) were obtained from Aldrich Chemicals and used as received. The ultra-pure (Milli Q) water was used to prepare experimental solutions. An aqueous  $\text{H}_2\text{SO}_4$  or NaOH solution was used for adjusting the pH of the solution before irradiation.

### 2.2. Analytical methods

Fourier transform-infrared (FT-IR) absorption spectra were recorded on a Thermo Nicolet Nexus 6700 instrument. The crystal phase analysis was done by a wide-angle X-ray diffraction (XRD) (Bruker D2 Phaser, USA) at 10 mA current and 30 kV voltage with a monochromatic  $\text{CuK}\alpha$  radiation ( $\lambda = 1.5405 \text{ \AA}$ ) with a  $2\theta$  step of  $0.05^\circ$  per 1 s, and a scan range of  $2\theta = 20\text{--}80^\circ$ . On an observation with a JEOL JSM-6500F cold field emission scanning electron microscope (FE-SEM), the samples were mounted on a gold platform placed in chamber. The transmission electron microscopic (TEM) observation was carried out on a Hitachi H-7000, Japan, with an acceleration voltage of 100 kV. The specimens were prepared by depositing a drop of the suspension of sample powder, which was ultrasonically dispersed in acetone for 10 min, on a carbon-coated copper grid, followed by drying at room temperature. The ultraviolet-visible absorption spectra were recorded using a Jasco V-670 series UV spectrometer. For the measurement of diffuse reflectance spectra (DRS), the powder sample was dispersed in acetone and the quartz plate was dipped in the concentrated dispersion and dried in an air.

### 2.3. Synthesis of dendrimer-ZnO nanocomposite

ZnO was prepared by simple physical grinding of zinc acetate with sodium hydroxide using pestle and mortar (Scheme S1, see Supplementary data) under solvent free condition. About 5 mmol (0.9174 g) of zinc acetate dihydrate was taken in mortar, and 20 mmol (0.8 g) of sodium hydroxide pellets were added. Then the mixture was ground in a mortar with pestle at room temperature. The grinding was continued for 1 h with 5 min interval for each

10 min. The formed zinc hydroxide was washed several times with water and ethanol, filtered and dried at room temperature for one day. The crystals were calcined for 3 h at  $200^\circ\text{C}$  in the muffle furnace heated at the rate of  $20^\circ\text{C min}^{-1}$ .

About 100 mg of ZnO nano rods were dispersed in 10 mL of ethanol under ultrasonication for 10 min, followed by addition of 100 mg of GPTMS to this solution (Scheme 1). After ultrasonication for 3 h, the unreacted GPTMS was removed by centrifugation. The precipitate of GPTMS-modified ZnO was washed three times with ethanol to complete removal of unreacted GPTMS.

About 100 mg of surface modified ZnO nano rods were dispersed in 20 mL of ethanol and  $10 \mu\text{L}$  of G4-PAMAM dendrimer was added to the dispersion. The mixture was stirred for 6 h at  $50^\circ\text{C}$  (Scheme 1). The chemically modified dendrimer-ZnO nanocomposite was collected by centrifugation and dried in air for one day.

### 2.4. Photodegradation experiments

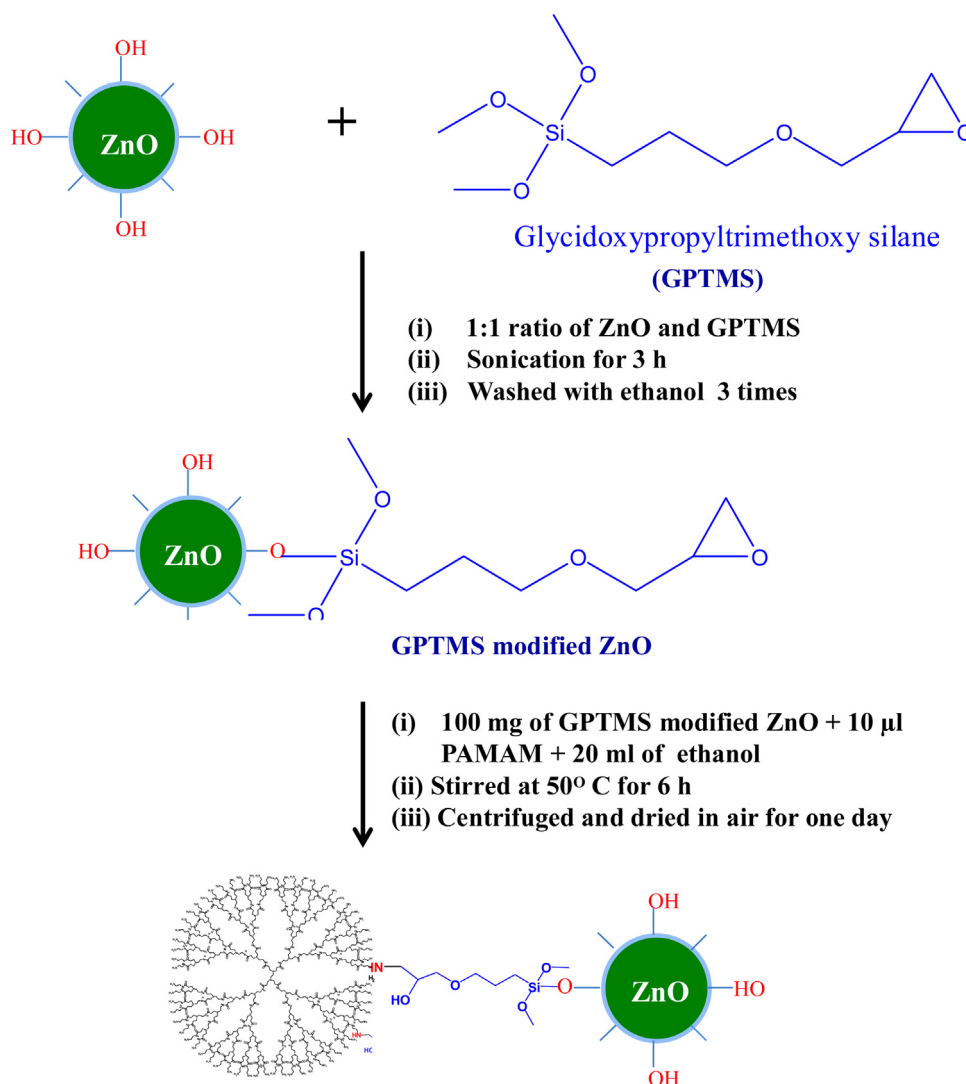
Photocatalytic activities of the as-obtained photocatalysts were evaluated by the degradation of NBB azo dye under a HOYA-SCHOTT Ex 250 photoreactor (UV light source  $<400 \text{ nm}$ ). In each experiment, the reaction suspension containing photocatalyst (10 mg) in a 50 mL NBB solution (30 ppm) was magnetically stirred in the dark for 30 min to ensure the adsorption equilibrium between photocatalyst powders and NBB. Then the solution was exposed to the UV light irradiation, and aliquots (4 mL) were sampled at given time intervals and centrifuged to remove photocatalyst powders. The filtrates were analyzed by recording the absorbance variations for an absorption band (320 nm) of NBB.

## 3. Results and discussion

### 3.1. Characterization of catalyst

The prepared ZnO nano rods and dendrimer-ZnO nanocomposite were characterized by different characterization techniques. XRD patterns of ZnO nano rod and dendrimer-ZnO nanocomposite are shown in Fig. 1. The diffraction peaks of ZnO (Fig. 1a) at  $31.66^\circ$ ,  $34.35^\circ$ ,  $36.13^\circ$  and  $56.47^\circ$  correspond to (100), (002), (101) and (110) planes of wurtzite ZnO (JCPDS 89-0511). The diffraction pattern of dendrimer-ZnO nanocomposite has no difference from that of ZnO nano rods, as shown in Fig. 1b. This reveals that dendrimer-ZnO nanocomposite has a wurtzite structure as well as ZnO nano rods without any disturbance by dendrimer. IR studies were performed to investigate the presence of PAMAM dendrimer in ZnO. The IR spectra of ZnO nano rods and dendrimer-ZnO nanocomposite are given in Fig. 2a and b, respectively. Absorption bands at 3384, 1548 and  $1398 \text{ cm}^{-1}$  can be attributed to the characteristic bands of surface hydroxyls of ZnO in both cases [1]. There are three new bands at 3502, 3328 and  $1616 \text{ cm}^{-1}$  in dendrimer-ZnO nanocomposite (Fig. 2b), which can be attributed to the characteristic bands of free and hydrogen bonded amino ( $-\text{NH}_2$ ) and amide group (CONH) of G4-PAMAM dendrimer [30]. In addition, dendrimer-ZnO has a strong absorption band at  $1116 \text{ cm}^{-1}$  due to antisymmetric stretching vibration of O–Si–O framework from GPTMS coupling agent [31].

The morphology of ZnO nano rods and PAMAM-ZnO was observed by FE-SEM and TEM and the images are given in Fig. 3. Both ZnO and PAMAM-ZnO had rod like structure, but the size of the rods decreased after the chemical modification by PAMAM dendrimer. It may be due to sonication effect during the surface modification. Under sonication, the elongated rods may be broken to decrease in length. The length of the nano rods was from 100 to 300 nm and the width of the rods was approximately 20–40 nm, while the size of dendrimer-ZnO composite



**Scheme 1.** Surface modification of ZnO by dendrimer using GPTMS.

was slightly shorter (50–150 nm) and thicker (30–50 nm). Furthermore, the rods and nanocomposite had some surface roughness. These roughnesses are helpful to adsorb the dye on the surface of the catalyst and it may increase the photocatalytic activity.

The diffuse reflectance spectra (DRS) of ZnO nano rods and dendrimer-ZnO nanocomposite are shown in Fig. 4a and b, respectively. The loading of PAMAM dendrimer on ZnO caused a small red-shift in the absorption edge from 395 to 407 nm. This result can be interpreted as a possible evidence for favorable interaction between ZnO and PAMAM dendrimer. The band gap energies of ZnO nano rods and dendrimer-ZnO were found to be 3.13 and 3.04 eV, respectively. That is, the dendrimer-loading on ZnO decreases the band gap energy of ZnO.

### 3.2. Photodegradability of NBB

#### 3.2.1. Effect of dendrimer-loading

The loading effect of PAMAM dendrimer has been tested toward NBB azo dye degradation (30 ppm of dye; 10 mg of catalyst and pH of dye solution = 6.5). The degradation was carried out using ZnO nano rods and dendrimer-ZnO composite, and the results were plotted concentration of NBB vs time, as shown in Fig. 5. The NBB degradation was calculated from the decrease of absorbance of an

absorption band at 320 nm. When the experiment with dendrimer-ZnO was performed in the dark environment without UV light power, no degradation occurred (curve a). However, in dark environment without UV light, the decrease in dye concentration in bulk occurred for dendrimer-ZnO (19.3%) and bare ZnO (12%). It may be the adsorption of dye on surface of the catalysts. Negligible degradation (0.2%) was also observed, when the reaction without any catalyst was allowed in the presence of UV light (curve b). From these observations, it can be clearly noted that both light energy and photocatalysts are needed for the effective degradation of NBB. About 80% of degradation took place at 75 min irradiation with dendrimer-ZnO (curve c), whereas ZnO nano rod gave 70% (curve d) degradation under the same condition. Similar higher degradation was observed even 15–60 min irradiation with dendrimer-ZnO. This indicates that dendrimer-ZnO has higher efficiency toward NBB degradation than ZnO nano rods under UV light.

#### 3.2.2. Effect of solution pH

The pH is one of the important parameters which influence the photocatalytic activity. Therefore, it is better to study the effect of pH on photodegradation of NBB dye with dendrimer-ZnO under UV light. The degradation of NBB by dendrimer-ZnO was carried out at different initial pH of the dye solutions. It was found from

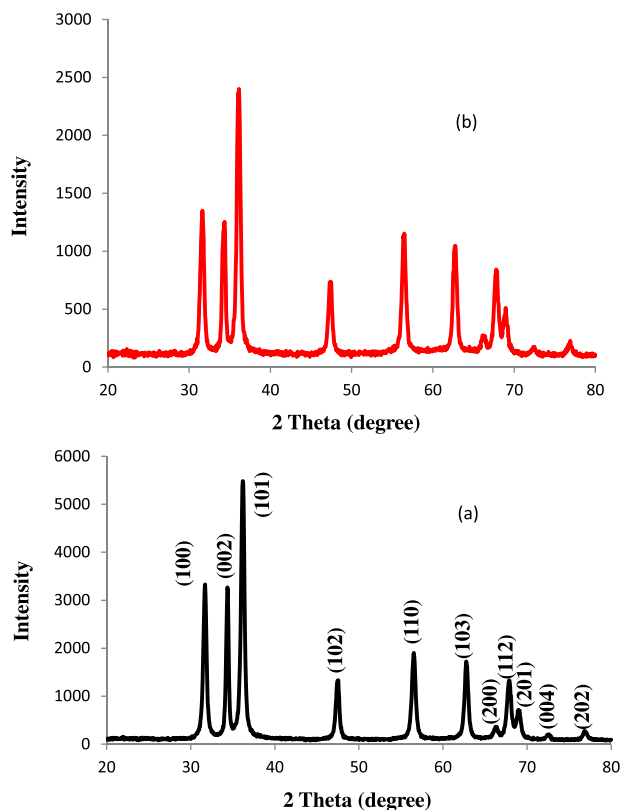


Fig. 1. XRD Patterns of (a) ZnO nano rods and (b) dendrimer-ZnO nanocomposite.

Fig. 6 that the degradation strongly depended on the solution pH. The degradation by dendrimer-ZnO at pH 4.0, 6.5 and 10.3 were 54.1, 63.9 and 72.0%, respectively, for 60 min irradiation, indicating that the efficient removal of NBB by dendrimer-ZnO is 8% higher

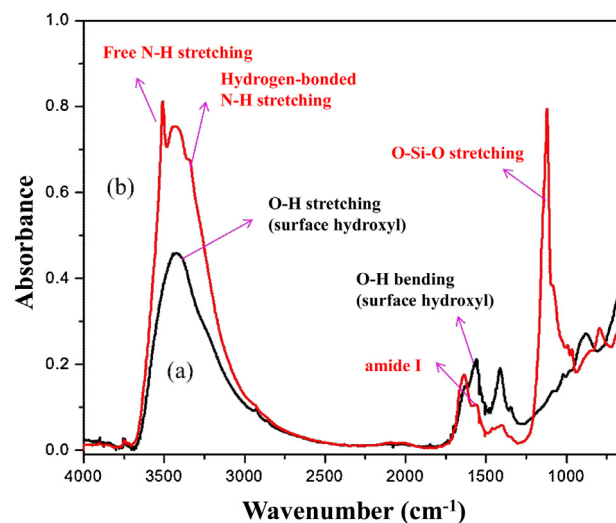


Fig. 2. IR spectra of (a) ZnO nano rods and (b) dendrimer-ZnO nanocomposite.

at pH 10.3 than at pH 6.5. Meanwhile, bare ZnO loses its activity in higher pH [32].

In order to achieve complete degradation at pH 10.3, the irradiation time was varied and the corresponding UV–vis spectra of an aqueous NBB (30 ppm) solution in the presence of dendrimer-ZnO are obtained at different irradiation time, as shown in Fig. 7. There was no significant change in absorption band positions during irradiation, but the absorbance of bands at 320 and 615 nm decreased gradually due to the degradation. It was also found that the degradation was reached 92.2% (12% higher than at pH 6.5) at 75 min irradiation and the complete degradation was achieved at 90 min irradiation for pH 10.3. This suggests that the degradation efficiency of dendrimer-ZnO is higher at high pH (10.3) than at pH 6.5 and that of bare ZnO. This is strong advantage for dendrimer-ZnO as a

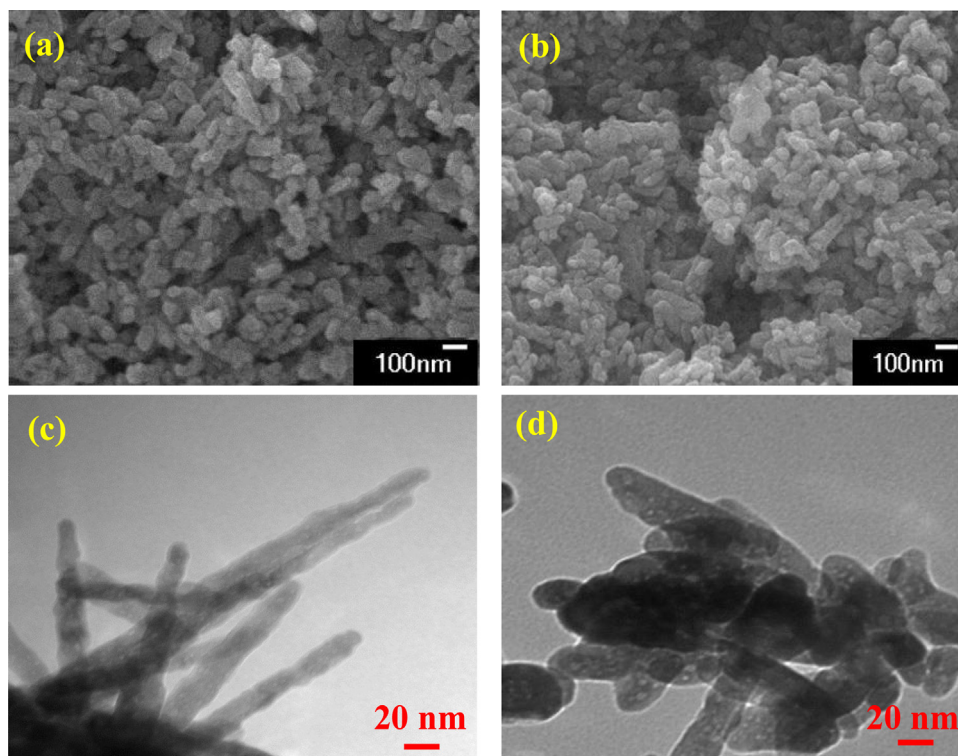


Fig. 3. FE-SEM images: (a) ZnO nano rods, (b) dendrimer-ZnO nanocomposite; TEM images: (c) ZnO nano rods, (d) dendrimer-ZnO nanocomposite.

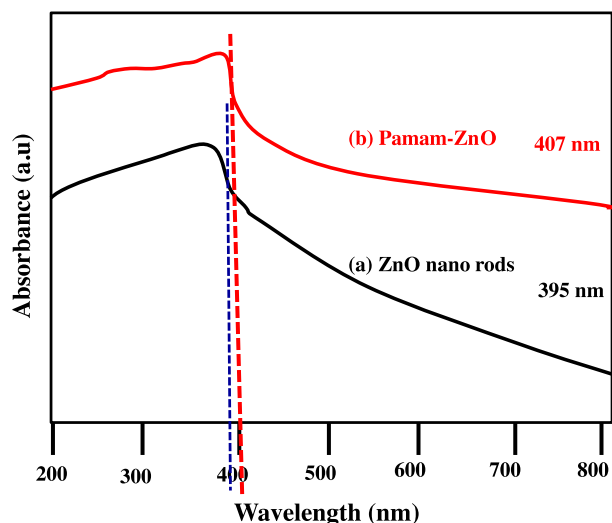


Fig. 4. DRS of (a) ZnO nano rods and (b) dendrimer-ZnO nanocomposite.

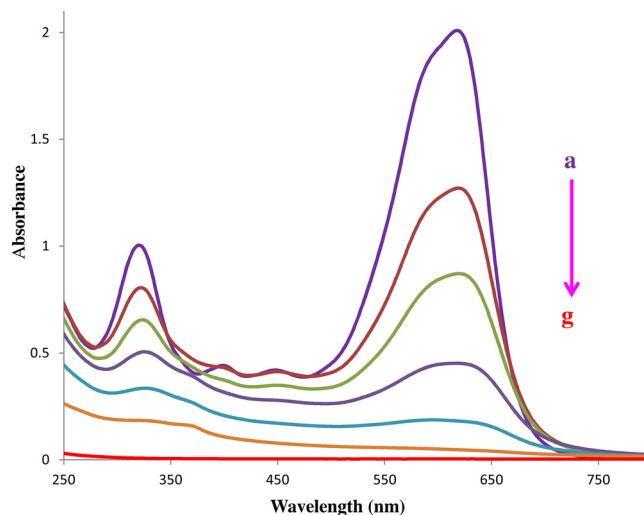


Fig. 7. UV-vis spectra of NBB after UV light irradiation in the presence of dendrimer-ZnO; [NBB] = 30 ppm, pH = 10.3, dendrimer-ZnO suspension = 10 mg/50 mL, irradiation time = (a) 0 min, (b) 15 min, (c) 30 min, (d) 45 min, (e) 60 min, (f) 75 min and (g) 90 min.

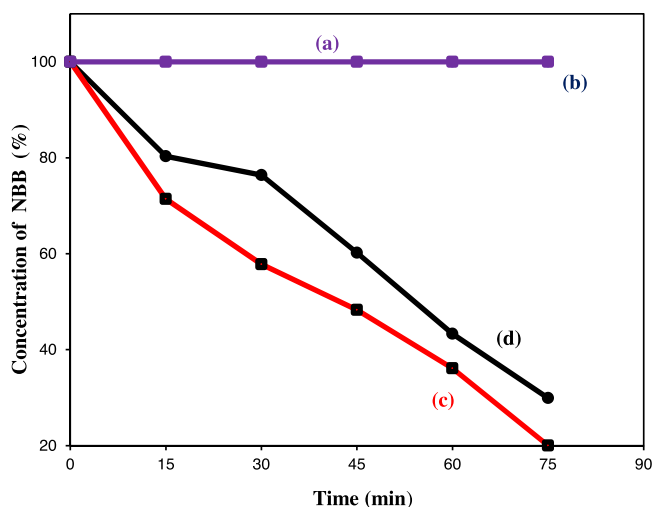


Fig. 5. Photodegradability of NBB; [NBB] = 30 ppm, catalyst suspension = 10 mg/50 mL, pH 6.5, (a) dendrimer-ZnO nanocomposite (dark, without irradiation), (b) no catalyst, (c) dendrimer-ZnO nanocomposite and (d) ZnO nano rods.

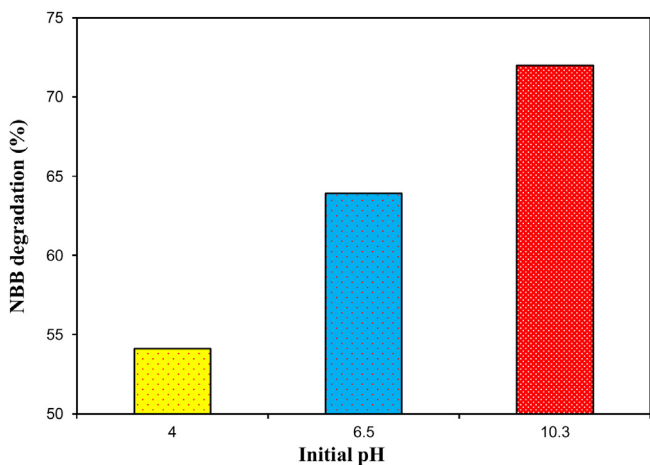


Fig. 6. Effect of solution pH; [NBB] = 30 ppm, dendrimer-ZnO suspension = 10 mg/50 mL, irradiation time = 60 min.

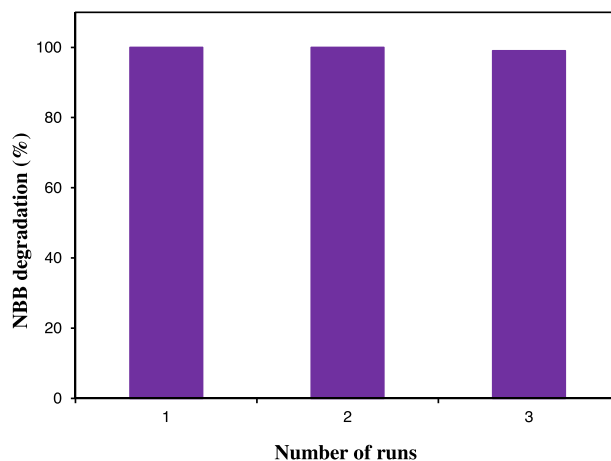
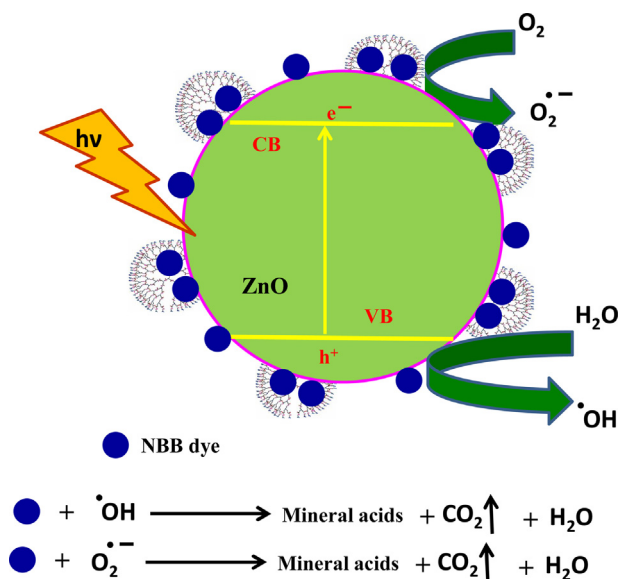


Fig. 8. Catalyst reusability; [NBB] = 30 ppm, dendrimer-ZnO suspension = 10 mg/50 mL, pH = 10.3, irradiation time = 90 min.

photocatalyst. It was already reported that AgBr-loaded ZnO was found to be very efficient toward NBB degradation at very high pH (pH 12) [3], although ZrS<sub>2</sub>-ZnO had the highest degradation effect at pH 6.5 [33]. The strong correlation of photocatalytic efficiency with the doping of guest (analyte) on catalyst surface has been reported for the system of dendrimer-protected TiO<sub>2</sub> [2,34]. The less removal efficiency at high acidic pH range is due to the reaction of charged ZnO with acids to produce the corresponding salt [3,5].

### 3.2.3. Stability of catalyst

In heterogeneous catalysis, the main advantage is the reusability of the catalyst. The catalyst reusability is an important performance of the photocatalytic process, because a significant cost reduction on the treatment of dye effluent is indispensable. When the catalyst was recycled owing to this reason, a drop in efficiency from 100% (1st run) to 99% (3rd run) was obtained as shown in Fig. 8. These results indicate that dendrimer-ZnO catalyst remains effective and reusable under UV light. Earlier, nano-chain ZnO and modified ZnO have been reported to have preferable antiphotocorrosive nature [5,35]. Thus, supposed that dendrimer-ZnO is antiphotocorrosive, this may be the reason for its reusability and photostability.



**Scheme 2.** Mechanism of degradation of NBB by dendrimer-ZnO nanocomposite.

### 3.2.4. Mechanism of photocatalytic degradation

The charge separation and photocatalytic reaction on dendrimer-ZnO photocatalyst are shown in Scheme 2. When semiconductor is illuminated by UV irradiation, a valence band (VB) electron goes to conduction band (CB), leaving a hole in valence band. The conduction band electrons are reacted with oxygen to produce superoxide radical anion, while the valence band holes are reacted with water to produce hydroxyl radical. Both species are very reactive toward NBB degradation. It was found that dendrimer-ZnO nanocomposite was more efficient for NBB degradation than ZnO nano rods. It could be expected that the hydrophilization by binding of PAMAM dendrimer enhances the adsorption of dye molecule on the surface of ZnO. Moreover, since PAMAM dendrimer can act as a reservoir of guest molecules, it may increase the number of NBB dye molecules close to the surface of ZnO. Similar result has been reported for dendrimer-protected TiO<sub>2</sub> toward 2,4-dichlorophenoxyacetic acid degradation [2]. The CB position of ZnO is more negative than the standard redox potential  $E^\circ = (\text{O}_2/\text{O}_2^{\cdot-})$  ( $-0.33$  eV vs NHE) [36], suggesting that electrons at CB of ZnO can reduce O<sub>2</sub> to O<sub>2</sub><sup>•-</sup>. In the same way, VB of ZnO is more positive than the standard redox potential  $E^\circ = (\text{OH}^-/\text{OH}^\cdot)$  ( $1.99$  eV vs NHE) [37]. This suggests that the generated holes in the VB of ZnO can oxidize OH<sup>-</sup> or H<sub>2</sub>O to form OH<sup>•</sup>, then involving the photocatalytic degradation of NBB.

## 4. Conclusion

Chemically modified dendrimer-ZnO was prepared for the first time. Initially, ZnO nano rods were prepared by simple physical grinding using pestle and mortar under solvent free condition. Then its surface was modified using a GPTMS binding agent and chemically bound with G4-PAMAM dendrimer to produce dendrimer-ZnO nanocomposite. The chemically modified dendrimer-ZnO nanocomposite was characterized by different techniques. XRD revealed the formation of wurtzite ZnO. TEM images revealed the formation of nano rods with surface roughness. It should be noted that dendrimer-ZnO was more efficient than ZnO nano rods for the degradation of NBB under UV light. The optimum pH for efficient removal of dye was 10.3. Reusability of this catalyst will make the treatment of dye effluent more

cost-effective. A degradation mechanism was proposed for higher degradation efficiency of dendrimer-ZnO. Eventually, since the prepared dendrimer-ZnO had superior photocatalytic activity toward the degradation of NBB at high pH, this procedure may be usable to the large scale treatment of industrial dye effluent which has high pH.

## Acknowledgement

This subject was financially supported by National Taiwan University of Science and Technology (103H237003). BK gratefully acknowledges National Taiwan University of Science and Technology, Taiwan, for the financial support by Postdoctoral Fellowship.

## Appendix A. Supplementary data

Supplementary data associated with this article can be found, in the online version, at <http://dx.doi.org/10.1016/j.apcata.2014.08.010>.

## References

- [1] R.Y. Hong, J.H. Li, L.L. Chen, D.Q. Liu, H.Z. Li, Y. Zheng, J. Ding, *Powder Technol.* 189 (2009) 426–432.
- [2] Y. Nakanishi, T. Imae, *J. Colloid Interface Sci.* 297 (2006) 122–129.
- [3] B. Krishnakumar, B. Subash, M. Swaminathan, *Sep. Purif. Technol.* 85 (2012) 35–44.
- [4] M. Long, Y. Qin, C. Chen, X. Guo, B. Tan, W. Cai, *J. Phys. Chem. C* 117 (2013) 16734–16741.
- [5] B. Subash, B. Krishnakumar, M. Swaminathan, M. Shanthi, *Langmuir* 29 (2013) 939–949.
- [6] C. Tian, W. Li, K. Pan, Q. Zhang, G. Tian, W. Zhou, H. Fu, *J. Solid State Chem.* 183 (2010) 2720–2725.
- [7] C. Wang, X. Wang, B. Xua, J. Zhaoc, B. Mai, P. Peng, G. Sheng, J. Fu, *J. Photochem. Photobiol. A* 168 (2004) 47–52.
- [8] A. Prasannan, T. Imae, *Ind. Eng. Chem. Res.* 52 (2013) 15673–15678.
- [9] S.H. Medina, M.E.H. El-Sayed, *Chem. Rev.* 109 (2009) 3141–3157.
- [10] Y. Cheng, Z. Xu, M. Ma, T. Xu, *J. Pharm. Sci.* 97 (2008) 123–143.
- [11] R.W.J. Scott, O.M. Wilson, R.M. Crooks, *J. Phys. Chem. B* 109 (2005) 692–704.
- [12] A. Buczkowski, P. Urbaniak, B. Palecz, *J. Mol. Liq.* 186 (2013) 70–75.
- [13] P.K. Maiti, T. Cagin, G. Wang, W.A. Goddard, *Macromolecules* 37 (2004) 6236–6254.
- [14] R. Esfand, D.A. Tomalia, *Drug Discov. Today* 6 (2001) 427–436.
- [15] D.A. Tomalia, *Prog. Polym. Sci.* 30 (2005) 294–324.
- [16] A. Siriviriyannun, T. Imae, N. Nagatani, *Anal. Biochem.* 443 (2013) 169–171.
- [17] A. Akyol, H.C. Yatmaz, M. Bayramoglu, *Appl. Catal. B* 54 (2004) 19–24.
- [18] B. Krishnakumar, M. Swaminathan, *Spectrochim. Acta A* 81 (2011) 739–744.
- [19] B. Krishnakumar, K. Selvam, R. Velmurugan, M. Swaminathan, *Desalin. Water Treat.* 24 (2010) 132–139.
- [20] N. Daneshvar, D. Salari, A.R. Khataee, *J. Photochem. Photobiol. A* 162 (2004) 317–322.
- [21] Z.L. Wang, *Today* 7 (2004) 26–33.
- [22] T. Iwasaki, M. Satoh, T. Masuda, T. Fujita, *J. Mater. Sci.* 35 (2000) 4025–4029.
- [23] C. Wang, O. Ranasingha, S. Natesakhawat, P.R. Ohodnicki Jr., M. Andio, J.P. Lewis, C. Matranga, *Nanoscale* 5 (2013) 6968–6974.
- [24] R. Ullah, J. Dutta, *J. Hazard. Mater.* 156 (2008) 194–200.
- [25] R. Wang, J. Guo, D. Chen, Y. Miao, J. Pan, W.W. Tjui, T. Liu, *J. Mater. Chem.* 21 (2011) 19375–19380.
- [26] M. Lou, D. Wang, W. Huang, D. Chen, B. Liu, *J. Magn. Mater.* 305 (2006) 83–90.
- [27] H. Li, Z. Zhang, X. Ma, M. Hu, X. Wang, P. Fan, *Surf. Coat. Technol.* 201 (2007) 5269–5272.
- [28] F. Grasset, N. Saito, D. Li, D. Park, I. Sakaguchi, N. Ohashi, H. Haneda, T. Roisnel, S. Mornet, E. Duguet, *J. Alloys Compd.* 360 (2003) 298–311.
- [29] M. Kathalewar, A. Sabnis, G. Waghoo, *Prog. Org. Coat.* 76 (2013) 1215–1229.
- [30] M. Ito, T. Imae, K. Aoi, K. Tsutsumiuchi, H. Noda, M. Okada, *Langmuir* 18 (2002) 9757–9764.
- [31] D. Onoshima, T. Imae, *Soft Matter* 2 (2006) 141–148.
- [32] B. Krishnakumar, M. Swaminathan, *Desalin. Water Treat.* 51 (2013) 6572–6579.
- [33] B. Krishnakumar, T. Imae, J. Mirac, J. Esquena, *Sep. Purif. Technol.* 132 (2014) 281–288.
- [34] Y. Nakanishi, T. Imae, *J. Colloid Interface Sci.* 285 (2005) 158–162.
- [35] R. Velmurugan, K. Selvam, B. Krishnakumar, M. Swaminathan, *Sep. Purif. Technol.* 80 (2011) 119–124.
- [36] Z. Li, Z. Xie, Y. Zhang, L. Wu, X. Wang, X. Fu, *J. Phys. Chem. C* 111 (2007) 18348–18352.
- [37] W. Liu, M. Wang, C. Xu, S. Chen, X. Fu, *Mater. Res. Bull.* 48 (2013) 106–113.